

# Fatigue Testing of Stiffened Traffic Signal Structures

Jay A. Puckett, Ph.D., P.E., M.ASCE<sup>1</sup>; Robert G. Erikson, Ph.D.<sup>2</sup>; and John P. Peiffer<sup>3</sup>

**Abstract:** Based on in-service inspection of poles with traditional designs, the inventory of Wyoming Department of Transportation (WYDOT) exhibited approximately a one-third cracking rate. A ring-stiffened connection is presently used. Sixteen fatigue tests were performed on 12 ring-stiffened cantilevered traffic signal pole connections to quantify the fatigue resistance. Two pole sizes were tested in three loading configurations: in plane, out of plane, and diagonal. Cyclic loading was applied to produce stress ranges (SRs) at several levels up to 16 ksi in the main member, more than six times the SR observed during monitoring an in-service pole. The WYDOT stiffened connection appears to be adequate to resist Wyoming's sustained winds that average approximately 12 mph in many locations. The possibility of using this connection with longer mast arms exists. Connection bolt fatigue failures were observed and may be the limiting fatigue design feature and important for inspection.

**DOI:** 10.1061/(ASCE)ST.1943-541X.0000229

**CE Database subject headings:** Traffic signals; Fatigue; Welds; Connections.

**Author keywords:** Traffic signal structure; Fatigue; Fatigue testing; AASHTO; Welded connection.

## Introduction

Fatigue life is a major consideration in the design of cantilevered traffic signal poles. The governing code for traffic signal structures is the American Association of State Highway and Transportation Officials' *Standard Specifications for Structural Supports for Highway Signs, Luminaires and Traffic Signals*, 4th Edition, 2001 (referred to as "AASHTO specifications" for the remainder of this paper). The AASHTO specifications require "infinite life" fatigue design for all overhead cantilevered traffic structures. Nominal stresses must not exceed the allowable constant-amplitude fatigue threshold, or endurance limit, of the detail. The constant-amplitude fatigue threshold varies throughout the structure based on the types of stresses carried and the fatigue resistance of a particular physical configuration (AASHTO 2001a,b).

Recent fatigue-related failures of cantilevered traffic structures and high-mast lighting towers have prompted research, field inspections, and design changes throughout the United States. Because of the failure of cantilevered traffic signal poles in Wyoming, the Wyoming Department of Transportation (WYDOT) is currently using a stiffened built-up box connection. Based on prior research at the University of Wyoming (UW) the ring-stiffened box connection (Fig. 1) is expected to perform significantly better under fatigue loading than a standard box connection (Hamilton et al. 2002). The project goal was to characterize the

constant-amplitude fatigue threshold for the stiffened box connection and the complete joint penetration (CJP) groove weld of the mast arms.

Full-scale virgin specimens were obtained from Valmont Industries. Twelve stiffened specimens, six each of the two different pole sizes, were tested in the Kester Structural Research Laboratory at UW. Basic pole and arm characteristics are given in Table 1. These two pole sizes are typical for new installations by WYDOT, with the large pole being the most commonly used (Paul Huck, Wyoming Department of Transportation, Office of the State Bridge Engineer, personal communication, August 2007).

Cyclic loads were applied to the test specimens in three different configurations: in plane, out of plane, and diagonal (see Fig. 2). The loading configurations were chosen for several reasons. First, the AASHTO specifications require the calculation of design loads and moments in the in-plane and out-of-plane directions. Thus, a correlation exists between the testing loads and the design loads. Second, previous research at UW has shown that these laboratory loading configurations are representative of actual in-service conditions. In addition, the diagonal configuration represents the simultaneous effects of in-plane and out-of-plane service loadings, which may be critical to the fatigue resistance of box connections (Hamilton et al. 2002).

A MTS testing system using servocontrolled hydraulic actuators provided constant force amplitude cyclic loading. To determine the required testing load, a nominal bending stress calculation was done for each loading configuration at a point in the main member located 1 ft below the point of intersection of the main member and the branching member (hereafter referred to as the "design point") (see Fig. 1). Per AASHTO specifications, for an untested connection, the nominal stresses in the main member "just below the connection of the branching member" shall not exceed stress Category E (4.5 ksi). A distance of 1 ft for the design point was chosen for convenience and uniformity (see Fig. 1).

Current test results typically plot above an AASHTO detail stress Category D (7 ksi) for design stresses at the design point. A summary of the constant-amplitude fatigue thresholds is readily

<sup>1</sup>V.O. Smith Professor, Dept. of Civil and Architectural Engineering, Univ. of Wyoming, Laramie, WY 82071 (corresponding author).

<sup>2</sup>Lecturer, Dept. of Civil and Architectural Engineering, Univ. of Wyoming, Laramie, WY 82071.

<sup>3</sup>Structural Engineer, MGA Structural Engineers, Inc., Colorado Springs, CO.

Note. This manuscript was submitted on June 30, 2009; approved on April 5, 2010; published online on April 9, 2010. Discussion period open until March 1, 2011; separate discussions must be submitted for individual papers. This paper is part of the *Journal of Structural Engineering*, Vol. 136, No. 10, October 1, 2010. ©ASCE, ISSN 0733-9445/2010/10-1205-1214/\$25.00.

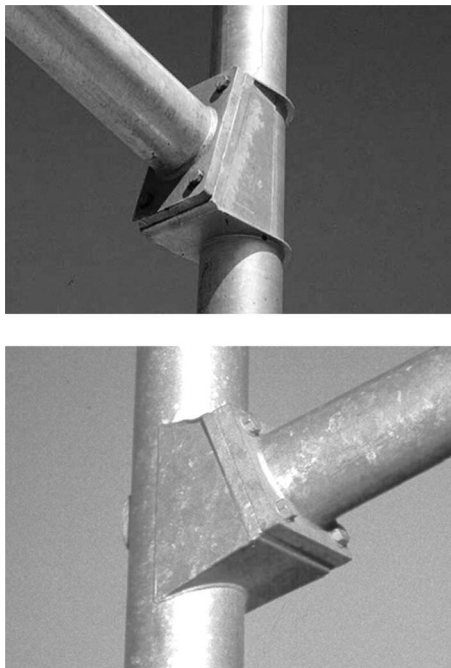


**Fig. 1.** Ring-stiffened connection, standard box connection

available in the 2001 AASHTO specifications, and their application to cantilevered traffic poles with box connections is summarized in Fig. 3 and plotted in Fig. 8. An analysis of nominal stresses in the WYDOT box connection shows that the controlling stresses occur at the design point.

## Background

Studies related to fatigue in the traffic signal poles span approximately two decades. The most comprehensive studies include work by National Cooperative Highway Research Program (NCHRP) projects (Dexter and Ricker 2002; Kaczinski et al. 1998; Connor and Hodgson 2006; Connor et al. 2005; Koenigs et al. 2003; Frank et al. 2007). All contain literature summaries related to traffic signal and/or high-mast poles. The *S-N* curve employed by AASHTO (2001a,b, 2007) has genesis in seminal work by Fisher and his many colleagues (Fisher et al. 1970, 1974). Recently Puckett and Barker in NCHRP 20-07(209) re-wrote many of the fatigue-related articles for consideration by AASHTO T-12, who is in charged with leading the specification development for AASHTO in 2001. The NCHRP 20-07(209) modifications were adopted by AASHTO in 2007 based on re-



**Fig. 2.** In-plane, out-of-plane, and diagonal loading configurations

search performed to date, where appropriate, in collaboration with T-12.

Current fatigue testing work is being conducted at University of Texas at Austin, Lehigh University, and Purdue University.

**Table 1.** Test Specimen Description

| Quantity | Specimen name | Base OD (in.), Fig. 3 | Top OD (in.), Fig. 3 | Wall thickness (in.), Fig. 3 | Overall length (ft), Fig. 3 | Pole OD at design point (in.), Fig. 5 | Material (ASTM) | Cross-sectional shape | Base/flange plate size (in. × in.), Fig. 3 |
|----------|---------------|-----------------------|----------------------|------------------------------|-----------------------------|---------------------------------------|-----------------|-----------------------|--|
| 6        | Small pole    | 11.52                 | 9.70                 | 0.2391                       | 13                          | 10.12                                 | A595, grade A   | Round                 | 14 × 20                                    |
| 6        | Large pole    | 14.30                 | 12.48                | 0.3125                       | 13                          | 12.90                                 | A572, grade 65  | 16 sided              | 17 × 27                                    |
| 4        | Small arm     | 12.00                 | 10.88                | 0.3125                       | 8                           | n/a                                   | A572, grade 65  | 12 sided              | 14 × 20                                    |
| 4        | Large arm     | 12.00                 | 10.88                | 0.3125                       | 8                           | n/a                                   | A572, grade 65  | 12 sided              | 17 × 27                                    |

Note: 1 in.=2.54 cm and 1 ft=0.3048 m.

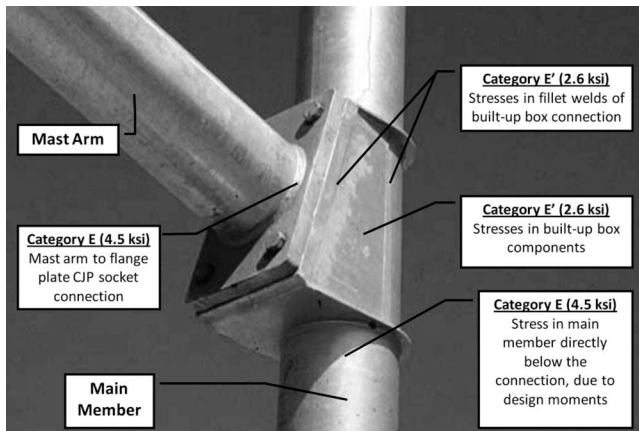


**Fig. 3.** AASHTO fatigue categories

This project adds to the database being develop across the United States.

### Description of Test Configuration

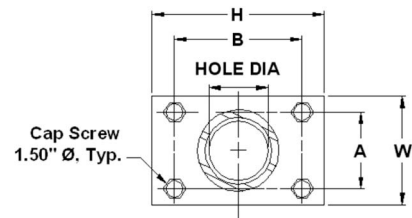
#### Test Specimens

Two sizes of pole specimens are described in Table 1. A flange plate of A36 steel, matching the size of either the small or large box connection, was welded to the arm with a full-penetration groove weld; the detail is shown in Fig. 4. The flange plate sizes for both box connections are given in Fig. 5.

Cycle counts and stress ranges (SRs) for the arms were recorded, so the performance of the full-penetration weld of the arm could be characterized as a secondary goal of this project.

The cross-sectional shapes of the poles and arms varied depending on the manufacturing process used. The large poles were 16 sided, the arms were 12 sided, and the small poles were round. All parts, including the bolts, were hot dip galvanized per ASTM A123 and A153. The connection bolts were 1-1/2 in. diameter grade A325 structural bolts. All poles and arms were tapered on their diameters at 0.14 in./ft. of length. For laboratory testing purposes, the poles and arms were manufactured at lengths of 13 and 8 ft, respectively.

Fillet weld profiles for each pole were recorded for four points around the circumference of the poles at the two circumferential



| SIGNAL ARM ATTACHMENT DATA |        |        |               |        |        |                           |
|----------------------------|--------|--------|---------------|--------|--------|---------------------------|
| Connection Size            | A [in] | B [in] | HOLE DIA [in] | H [in] | W [in] | Base Plate Thickness [in] |
| Small Box                  | 9.5    | 13     | 10.4          | 20     | 14     | 1.5                       |
| Large Box                  | 12     | 20     | 10.4          | 27     | 17     | 2.0                       |

**Fig. 5.** Arm flange plate dimensions (WYDOT 2005)

fillet welds and at four places around the circumference of the arm socket connection. Weld profile sets for all poles and arms are provided by Peiffer et al. (2008).

For the circumferential fillet welds that were profiled, the WYDOT specification is a 5/16 in. fillet weld, noted in Fig. 6. The average actual fillet weld size of all specimens was 0.442 in., about 1/8 in. greater than specified. A comparison was done by measuring and averaging the throat distance of all of the specimens and dividing it by the cosine of 45° to obtain an equivalent fillet leg length. This method avoided an inaccurate direct fillet leg length measurement because many of the actual fillet profiles are concave in shape. A possible explanation for the deviation between actual and specified fillet sizes is Note 5 of the WYDOT specification, which states, “Ensure the radial separation between the face of the pole and the adjacent inside face of the top or bottom gusset plate does not exceed 3/16”. If the separation is greater than 1/16”, increase the leg of the fillet weld by the amount of the separation.” The gusset plate referred to in here is the stiffener ring. Thus, the actual fillet size is dependent on the supplier’s chosen process and tolerance for manufacturing the stiffener.

Comparisons of specified to actual fillet weld sizes at other locations of the box connection are as follows:

- Side plate welds—specified as a 5/16-in. equal leg fillet. The actual fillet weld is unequal in leg length with the range vary-

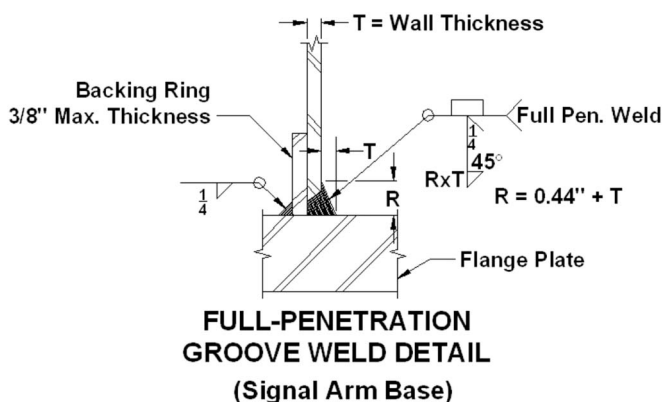


**Fig. 4.** Full-penetration groove weld detail between the arm and the flange plate (WYDOT 2005)

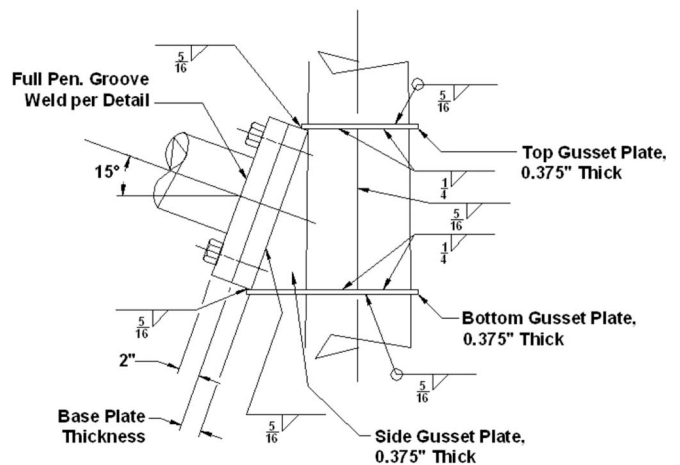


**Fig. 6.** Weld specifications for large and small box connections (WYDOT 2005)

ing from 1/4 to 9/16 in. The most common fillet size is 5/16 × 3/8 in. leg lengths.

- Base plate welds—specified as a 5/16 in. fillet. The actual size range varies from 1/4 to 3/8 in., with the most common size being 3/8 in.

### Testing System

MTS actuators for all tests were 55-kip capacity with a stroke of 6 in. Calibration of the load cells and linear potentiometers was performed by the original equipment manufacturer before testing began. A load cell calibration tolerance of 1% of the load set point was used.

The floor of the Kester Structures Lab is a 2-ft-thick slab of reinforced concrete, with basement access. A reaction wall, consisting of two 18 × 36 × 72 in. reinforced concrete blocks, provided a vertical surface for actuator attachment. The reaction wall assembly was restrained to the floor with two 1-1/2 in. diameter DYWIDAG threaded rods, each posttensioned to 100 kips.

A typical in-plane setup is illustrated in Fig. 2(a). Notice that the pole is in a horizontal orientation and the mast arm is 15° from vertical. This pole orientation was used for the out-of-plane and diagonal test configurations as well. The actuator, for in-plane configurations, is at 90° to the arm, measuring from its unloaded (neutral) position. The moment arm is the distance from the actuator to the design point, measuring parallel to the axis of the pole.

An example of the out-of-plane setup is given in Fig. 2(b). Here, the moment arm is the vertical distance from the point of intersection of the actuator axis and arm axis to the centerline of the pole. The diagonal test configuration is shown in Fig. 2(c). Moment arm lengths varied between tests and are given for each test on their respective data sheets, and details of stress computations are provided by Peiffer et al. (2008).

### Testing Regimen and Applied Loads

#### Applied Loads

The applied loads were computed based on flexural stresses at the design point (see Fig. 1). The method of determining the applied testing force is consistent with procedures used for design (AASHTO 2001a,b). Axial and torsional stresses are neglected and, from detailed calculations, are shown to affect the total principal stresses by less than 5%.

The testing amplitude of the actuator force to produce the desired SR is 1/2 of the computed load. The testing force amplitude is required to produce the desired SR at the design point. It is applied in both directions (push and pull) from the unloaded position of the arm. Detailed computations are available in Peiffer et al. (2008). Additionally, a summary of typical startup and operation procedures is described by Peiffer et al. (2008) as well.

#### Duration of Tests

A runout limit of 13-million cycles was chosen to ensure that the beginning of the constant-amplitude fatigue threshold for the E detail category was exceeded by at least 10%. The constant-amplitude fatigue threshold starts at approximately 11.5-million cycles for Category E. Because of time constraints, 10-million cycles were chosen as the runout limit for the out-of-plane and diagonal tests after Test 6.

Typically a log-log plot of AASHTO detail stress categories and their constant-amplitude fatigue thresholds is used. Because



Fig. 7. Dye penetrant results of fillet weld joint failure, Test 11

the chart was intended to be used for design, i.e., calculated nominal stresses shall be below an allowable value, the category values were conservatively chosen at the lower bound of the test data. The seminal works upon which these plots are based are NCHRP Reports 102 and 147. Herein Fisher et al. conducted hundreds of fatigue tests associated with steel bridge girders and associated weld details. The design values for the finite life portion of the chart were determined such that the detail has a 95% chance of failure with a confidence limit of also 95%. Sufficient data were available for statistical analysis. As the SR is set during a fatigue test and the dependent variable is the number of cycles to failure, the design curve was shifted to the left from the mean data. Based on data presented in Reports 102 and 147, it appears that an estimated shift is approximately 2/3 of the mean value (cycles). For example, a mean test value of 1-million cycles would have a design value of approximately 660,000 cycles. The variability of various details was similar and, in all cases, a normal distribution with log  $N$  was demonstrated. Fisher et al. did not address the constant amplitude fatigue life (CAFL) as this was not considered as part of the design procedure at this time (Fisher et al. 1970, 1974).

Thus, the mean number of cycles to failure is greater than that associated with stress category for design. The shift to the mean values may be estimated if desired. In the present work, the design  $S-N$  curves are used.

Tests 2 and 4 were “continued” tests at a higher stress level. Because no fatigue cracking was observed during Tests 1 and 3, the same poles were tested at a higher SR. An equivalent constant-amplitude stress range (CASR) was then calculated for the combined tests using the Palmgren-Miner rule. Several tests were terminated prior to reaching their predetermined runout limit; these are explained later.

#### Crack Inspection

Crack detection was performed with a commercially available dye penetrant. The basic procedures are provided elsewhere (Sherwin Incorporated 2005).

As noted earlier, the dye penetrant method has been shown to

**Table 2.** Summary of Pole Test Data

| Pole test number | Pole test ID  | Pole size       | Total cycles on pole  | CASR (ksi) | Weld fatigue failure (Y/N) | Plotted on <i>S-N</i> figure number | Comments  |
|------------------|---------------|-----------------|-----------------------|------------|----------------------------|-------------------------------------|---|
| 1                | 1L-IP-7.5     | Large           | 13,050,000            | 7.5        | N                          | 9                                   | Virgin pole and arm.<br>Test ended—no cracks detected.  |
|                  | 1S-IP-7.5     | Small           | 13,050,000            | 7.5        | N                          | 8                                   | Virgin pole and arm.<br>Test ended—no cracks detected.  |
| 2                | 2L-IP-16.0    | Large           | 13,188,000            | 7.7        | N                          | 11                                  | This test is a continuation of test 1L-IP-7.5, NSR increased.<br>Test ended—actuator malfunction.   |
|                  | 2S-IP-16.0    | Small           | 13,462,000            | 8.1        | N                          | 10                                  | This test is a continuation of test 1S-IP-7.5, NSR increased.<br>Test ended—clamping block failed.  |
| 3                | 3L-IP-7.5     | Large           | 13,000,000            | 7.5        | N                          | 9                                   | Virgin pole.<br>Test ended—no cracks detected.  |
|                  | 3S-IP-7.5     | Small           | 13,000,000            | 7.5        | N                          | 8                                   | Virgin pole.<br>Test ended—no cracks detected.  |
| 4                | 4L-IP-16.0    | Large           | 13,146,000            | 7.7        | N                          | 11                                  | This test is a continuation of test 3L-IP-7.5, NSR increased.<br>Test ended—pole wall fatigued within the front clamping block. One connection bolt failure.        |
|                  | 4S-IP-16.0    | Small           | 17,036,000            | 10.9       | N                          | 10                                  | This test is a continuation of test 3S-IP-7.5, NSR increased.<br>Test ended—pole wall fatigued within the front clamping block.                                     |
| 5                | 5L-IP-16.0    | Large           | 13,000,000            | 16.0       | N                          | 11                                  | Virgin pole. Test ended—no cracks detected.   |
|                  | 5S-IP-16.0    | Small           | 13,000,000            | 16.0       | N                          | 10                                  | Virgin pole. Test ended—no cracks detected.   |
| 6                | 6S-OP-7.5     | Small           | 13,000,000            | 3.1        | N                          | 8                                   | Virgin pole. Test ended—no cracks detected.   |
| 7                | 7S-OP-16.0    | Small           | 1,908,000             | 6.5        | N                          | 10                                  | Virgin pole. Pole wall cracked just inside the clamping block at torsion plate weld was repaired at 936,000 cycles and re-cracked through repair at current cycles. |
| 8                | 8L-OP-16.0    | Large           | 542,600               | 6.5        | N                          | 11                                  | Virgin pole. Pole wall cracked just inside the clamping block at torsion plate weld.  |
| 9                | 9S-DIAG-16.0  | Small           | 875,700               | 16.0       | N                          | 10                                  | Virgin pole. Pole wall cracked just inside the clamping block at torsion plate weld.  |
| 10               | 10L-OP-16.0   | Large           | 329,000<br>in process | 6.5        | Y                          | 11                                  | Virgin pole. Crack first observed at 1.9-million cycles. Lengthened to 5.2 in. with no appreciable increase in displacement. Test ended due to equipment failure.   |
| 11               | 11L-DIAG-16.0 | Large           | 10,000<br>in process  | 16.0       | Y                          | 11                                  | Virgin pole. Crack first observed at 2.78-million cycles. Sudden 120% increase in displacement.   |
| 1 in.=2.54 cm    |               | 1 ksi=6.895 MPa |                       | K=1,000    |                            | M=1,000,000                         |   |

be effective for traffic signal structures (Hamilton et al. 2002). However, the limitations of the procedure must be understood and the technique mastered to obtain reliable results. An example of a typical dye penetrant inspection is shown in Fig. 7.

## Results

### Fatigue Test Data

A summary of the pole test results is given in Table 2. “Pole test ID” labeling uses L and S for large and small connections, respectively. OP, IP, and DIAG indicate the load direction (see Fig. 2). The applied force is the actuator amplitude force; i.e., this force was applied equally in the push and pull directions from the neutral unstressed position. The applied force values may be different for the same size pole and the same SR because of changes in the moment arm length or actuator angles. In cases where the specimen test was continued after runout with an increased SR, the CASR may be slightly different from the primary test SR. The primary data are presented by Peiffer et al. (2008).

The in-plane SRs are computed based on the flexural bending moment divided by the section modulus of the pole at the design point. This calculation is straightforward. However, for the out-of-plane case, it is conventional to neglect the torsional load effects. For the out-of-plane tests, the applied moment (torque) was set to be the same as the flexural moment of the in-plane test of the same SR. This load also creates a flexural bending stress, and it is this nominal flexural bending stress computation that is used for the SR (see Peiffer et al. 2008). This computation is consistent with the design SR requirements of AASHTO (2001a,b). (Note that torsion creates a small shear stress in the weld near the design point and is neglected.) The applied out-of-plane moment that creates a nominal flexural stress of 3.1 ksi is associated with a 7.5-ksi in-plane SR. Similarly, the nominal out-of-plane flexural stress of 6.5 ksi is associated with the 16-ksi in-plane SR. In summary, the in-plane and out-of-plane moments for each test level are equal, though their SRs per se are not.

The actuator load for the diagonal test was set based on the vector combination of the in-plane and out-of-plane stresses. Table 3 contains data for arms that failed due to fatigue. The

**Table 3.** Arm Data (Raw)

| Arm ID     | Pole test ID  | Nominal stress range (ksi) | Cycles of test until arm failure |
|------------|---------------|----------------------------|----------------------------------|
| L-IP-001   | 1L-IP-7.5     | 6.4                        | 13,050,164                       |
|            | 2L-IP-16.0    | 13.6                       | 137,466                          |
|            | 3L-IP-7.5     | 6.4                        | 13,000,000                       |
| L-IP-002   | 4L-IP-16.0    | 13.6                       | 146,050                          |
|            | 5L-IP-16.0    | 13.6                       | 2,118,508                        |
|            | 5L-IP-16.0    | 13.6                       | 6,291,492                        |
| L-DIAG-004 | 11L-DIAG-16.0 | 11.2                       | 2,025,211                        |

Note: 1 in.=2.54 cm and 1 ksi=6.895 MPa.

nominal SR of an arm for a given test is different from the pole of the same test because of different section moduli and moment arms.

Fatigue testing of this type proves to be tough on equipment and fixtures. In cases for which the tests were stopped short of the desired runout, an explanation is provided in Table 2.

For the tests/components that experienced variable amplitudes, the Palmgren-Miner rule was used to determine the equivalent CASR. Here the combinational exponent used was one-third that is typical for steel welds (The Committee on Fatigue and Fracture Reliability of the Committee on Structural Safety and Reliability of the Structural Division 1982; Peiffer et al. 2008; AASHTO 2008).

**Table 4.** CASR-Adjusted Arm Data

| Arm ID           | CASR (ksi) | Cumulative cycles | Plotted on S-N figure number |
|------------------|------------|-------------------|------------------------------|
| 12-2005-L-IP-001 | 7.7        | 28,452,188        | 13                           |
| 08-2006-L-IP-002 | 13.6       | 6,291,492         | 13                           |

Note: 1 in.=2.54 cm and 1 ksi=6.895 MPa.

With regard to the secondary purpose of testing the detail category of CJP welds for the mast arms, the adjusted arm data are provided in Table 4. Also relevant is the small arm used in Tests 1–5 (S-IP-001) that accumulated 43.5-million cycles of in-plane loading at a 5.0-ksi CASR and did not experience fatigue failure.

### Miscellaneous Results and Findings

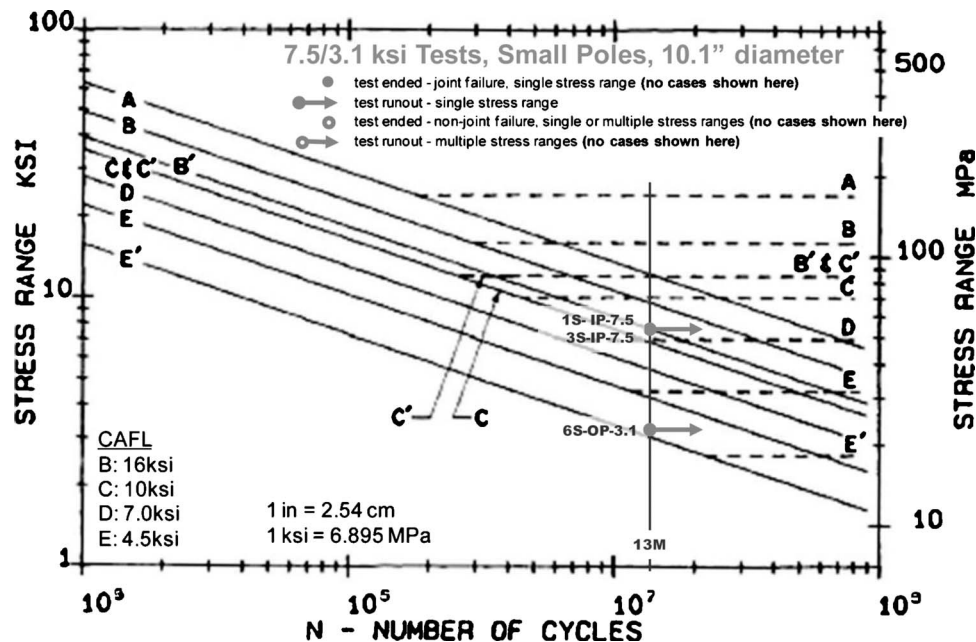
Four connection bolt fatigue failures occurred during Tests 4L-IP-16.0 and 5L-IP-16.0 and one failure for each of Tests 10L-OP-6.5 and 11L-DIAG-16.0. Calculated tensile forces are below AASHTO and AISC [American Institute of Steel Construction (AISC) 2001] specification constant-amplitude fatigue thresholds. Because test results contradicted this, a detailed bolt fatigue analysis was performed and is presented by Peiffer et al. (2008). Results show that the bolts do not have a sufficient safety factor and indicate that if the large box connection were used at a 16.0-ksi in-plane nominal SR, the limiting design feature may be the bolt fatigue life. However, a similar analysis of the small pole also gives an insufficient factor of safety; yet, no bolt failures occurred during small pole testing. The following two preliminary conclusions are suggested:

- Prying action caused by deformation of the arm flange plate under in-plane loads may be significant.
- Improper pretensioning of the connection bolts, perhaps due to curvature of the flange plate, results in an unexpected distribution of the load throughout the bolt-flange-plate system.

### Analysis of Results

#### Adjusted Test Data Plotted on AASHTO S-N Charts

The CASR and total number of cycles for each specimen from Table 2 are plotted on AASHTO S-N charts in Figs. 8–11. The data points are for nominal bending stresses at the design point

**Fig. 8.** Adjusted test data, small pole, 7.5/3.1 ksi

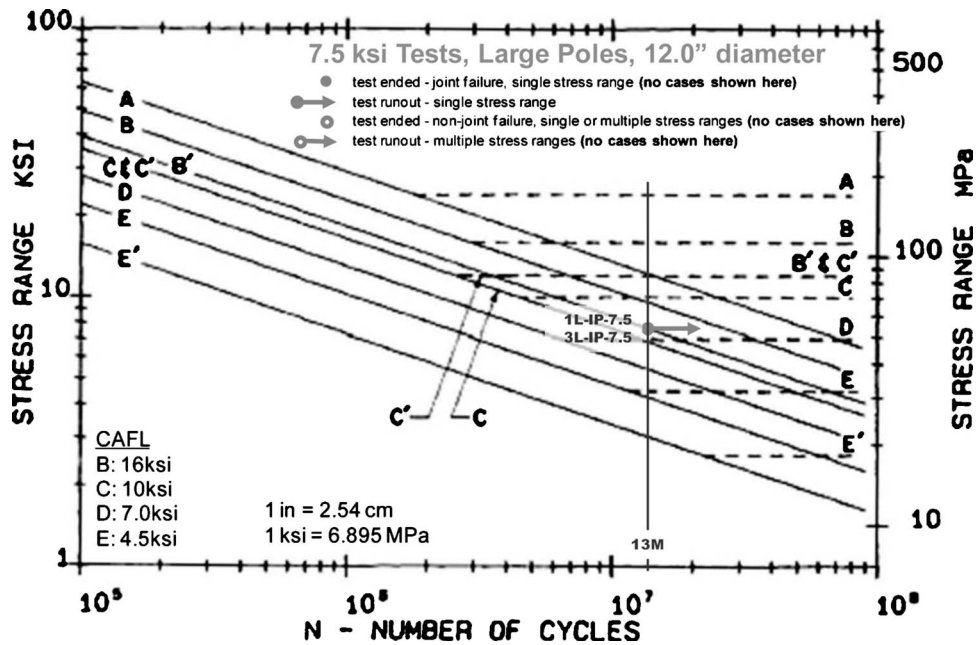


Fig. 9. Adjusted test data, large pole, 7.5 ksi

(see Fig. 1). For the two tests that experienced connection fatigue failure, the data point was plotted at the number of cycles at which crack was first observed.

For reference, a vertical line is marked at the 13-million cycle location. The outside diameter at the design point is provided on the charts. For readability, the pole test data are provided on four separate plots.

The adjusted arm data are plotted in Fig. 12, showing the three arms that failed due to fatigue (Table 4) and one that accumulated 43.5-million cycles and did not fail. The data points for the arms are for nominal bending stresses in the arm adjacent to the CJP weld.

### Comparison with S-N Curves

These tests were categorized according to the following:

1. Conclusive: Terminated prior to cycle runout with fatigue cracks.
2. Useful information about the lower bound: Terminated prior to cycle runout with no fatigue cracks, but the number of cycles greater than a CAFL.
3. Inconclusive: Terminated prior to cycle runout with no fatigue cracks and prior to reaching a CAFL (could be failure of fixture, etc.).

Thus, Test 8L-OP-6.5 (Fig. 11) is considered inconclusive.

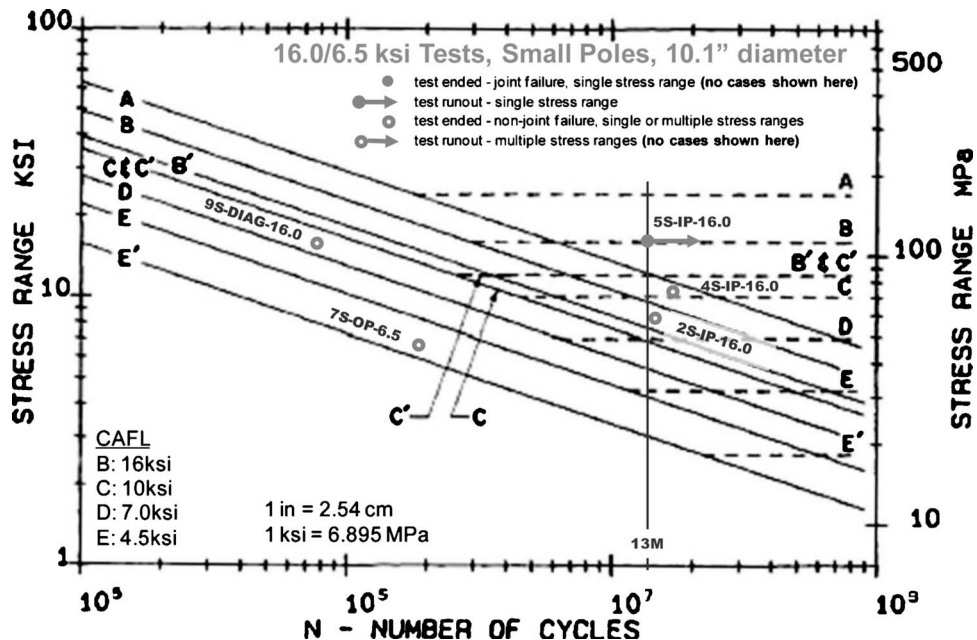


Fig. 10. Adjusted test data, small pole, 16.0/6.5 ksi

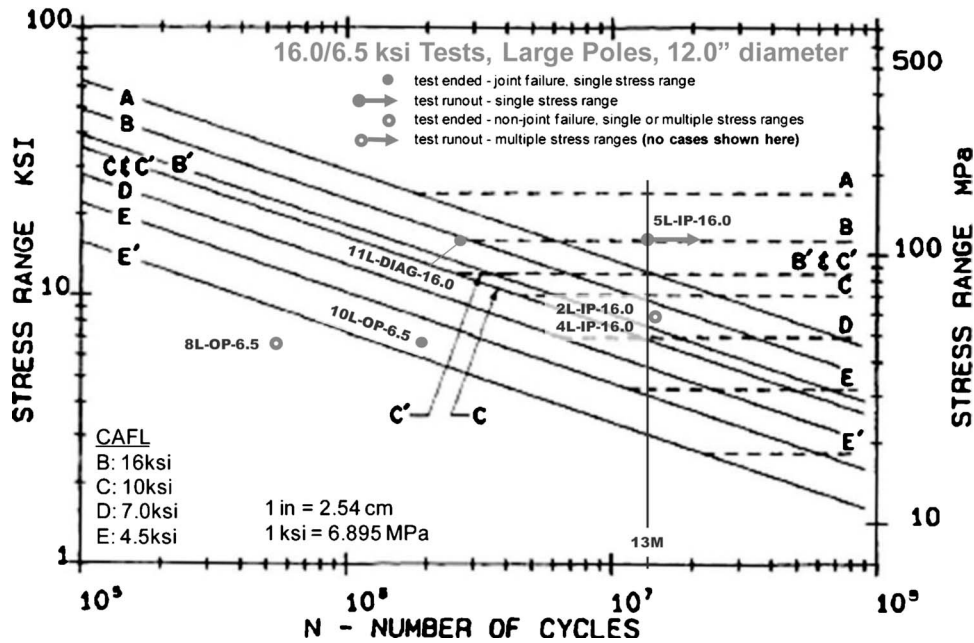


Fig. 11. Adjusted test data, large pole, 16.0/6.5 ksi

Tests 2L-IP-16.0 and 4L-IP-16.0 (Fig. 11) provide useful information regarding the allowable stress of the detail because the number of test cycles places the data point in the infinite life region of the plot, and no fatigue cracks were observed.

As described earlier, the AASHTO *S-N* charts are intended for design, and the mean number of cycles (test data) is approximately 50% greater than that permitted for design (Fisher et al. 1970, 1974). Shifting the number of cycles by this amount has a minor effect on the estimated fatigue category.

Other tests were completed to the desired cycle runout. Seven poles exhibited runouts above Category D (7.0 ksi). In addition, Test 11 plots above the Category B' curve (12.0 ksi) (see Fig. 11). Test 10 plots between E and E'. Note that the applied out-of-plane

moment for Test 10 is the same moment (torque) as the in-plane moments at the 16-ksi SR. Considering only the flexural component of the stress normal to the weld, the applied SR is approximately 6.5 ksi for Test 10. This stress is consistent with the manner in which the out-of-plane stress is computed for design (AASHTO 2001a,b).

The secondary objective was to quantify the detail category of the CJP weld of the mast arms shown in Fig. 4. Three CJP joint failures plot above the detail stress Category D (see Fig. 12). The small arm, S-IP-001, that did not experience fatigue cracks accumulated over 43-million cycle plots above a CAFL Category E (4.5 ksi).

Considering only the *in-plane* test results for the box connec-

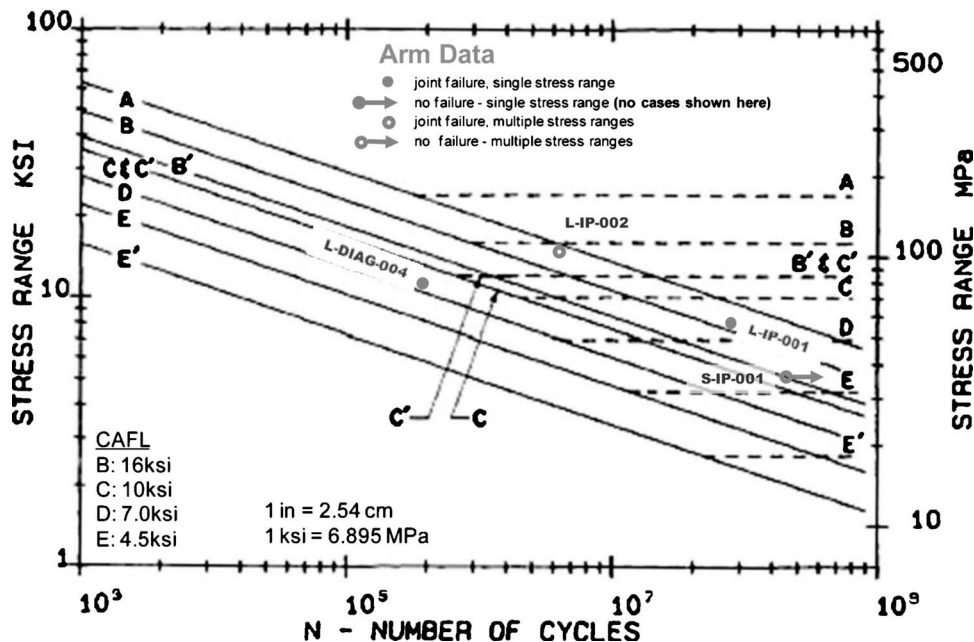


Fig. 12. Adjusted arm data

tion, there were seven poles tested at 7.5- or 16-ksi CASRs. None experienced a fatigue failure. However, if the ring-stiffened box connection is used at in-plane stresses approaching 16.0 ksi, the following limiting fatigue design factor may not be the box connection details rather

- Connection bolt fatigue;
- Internal thread fatigue seen in the large pole base plate; or
- Mast arm CJP weld fatigue.

Again, a SR=16 ksi is very high compared to in-service observations and design computations.

The nature of the fatigue crack propagation was different for each test. For the out-of-plane test, Test 10, the crack initiated at the toe of the second weld pass and increased in length to 5–1/8 in. over 500,000 cycles. The crack was first observed at 1.9-million cycles and did not increase appreciably in length for the duration of the test to 4.6-million cycles. The amplitude of the stroke at the test load of 4.33 kips also did not increase significantly throughout the entire test, even after the crack was observed. The crack propagated circumferentially 5–1/8 in. through the pole wall staying within the weld bead. Near the end of testing, the crack entered the pole wall and stiffener plate.

For the diagonal test (see Fig. 7), the crack initiated at the toe of the weld and increased in length to 4 in. over 300,000 cycles. The stroke amplitude more than doubled as the crack increased to its full length. The crack did not follow the toe of the weld but propagated through the ring stiffener, thus accounting for the large increase in displacement during the pull stroke that opens the crack. For fatigue design considerations with the ring-stiffened WYDOT connection, test results indicate that out-of-plane and diagonal loadings are more severe than in-plane loading at the same SR.

### Comparison with Observed Field CASR

The load effect of a design wind event, computed according to AASHTO specifications, is a peak stress that rarely occurs. Only 1 in 10,000 cycles (0.01% of all cycles) is expected to exceed the constant-amplitude fatigue threshold given by the AASHTO specifications (Dexter and Ricker 2002). Current research was conducted at constant-amplitude loading (for primary tests). Therefore, a valid comparison of laboratory-tested versus field-observed SRs is to consider the CASR in situ field findings from prior UW research. Details of this study are provided by Hamilton et al. (2002b) where methods and SR histograms are provided.

These CASR in-service loading data were collected over a time span of 38 months for an instrumented pole in Laramie, Wyo. The monitored structure is typical of the WYDOT inventory and poles used by many agencies. The average wind speed in Laramie is approximately 12 mph, and the pole was oriented perpendicular to the prevailing wind, which is critical. The investigators examined in-plane, out-of-plane, and the combined load effects. The worst case combined CASR for the main member design point is 2.48 ksi.

Current tests at 16.0 ksi are more than six times the observed field values. All tests exceeded this value. Based on current design practice, a SR of 16.0 ksi at the design point is severe loading. By this measure, the joint fatigue resistance is adequate.

### Summary

Based on in-service inspection of pole with traditional designs, Wyoming DOT's inventory exhibited approximately a one-third

cracking rate. A ring-stiffened connection is presently used.

Sixteen fatigue tests were performed on 12 ring-stiffened cantilevered traffic signal pole connections to quantify the fatigue resistance. Two pole sizes were tested in three loading configurations: in plane, out of plane, and diagonal.

A MTS testing system using servocontrolled hydraulic actuators provided constant force amplitude cyclic loading. To determine the required testing load, a nominal bending stress calculation was computed for each loading configuration at a point in the main member located 1 ft below the point of intersection of the main member and the branching member. Per AASHTO specifications, the nominal SR in the main member just below the connection of the branching member shall not exceed stress Category E (4.5 ksi). Current test results typically plot above an AASHTO detail stress Category D (7 ksi) for design stresses at the design point in most cases.

Wyoming winds are sustained with an average speed of approximately 12 mph, significantly greater than the national average. Such sustained winds create millions of fatigue cycles in Wyoming's traffic signal structures. A maximum CASR of 2.48 ksi was observed from in-service monitoring. Applied SRs significantly exceeded observed SRs. This provides another measure of the fatigue resistance relative to the expected demand.

Test results indicate that a properly designed ring-stiffened box connection will have a higher fatigue resistance than a standard box connection of the same size. Moreover, the critical regions to check SRs are in the mast arm-to-flange plate welded connection, the four connection bolts, and just below the box connection. There have been no signs of distress with the box connection. The box connection can be considered adequate by these performance tests.

### Limitations

This paper is limited to stiffened built-up box connection per WYDOT design specifications (WYDOT 2005). The test data are only valid for this stiffened box connection design and for the sizes tested. The data points plotted in Figs. 8–11 are for nominal bending stresses at the design point. Therefore, extrapolation for stresses at points in the box connection other than the design point, or for emulation of the WYDOT box connection for designs that appear to be similar, but not identical, is not recommended.

### Acknowledgments

The support of WYDOT engineers Gregg Fredrick, Paul Huck, and Jeff Booher is appreciated. They provided significant help in the design of the test matrix, setting the SR levels, and providing background and documentation on WYDOT design practice. Additionally, Gregg Fredrick was helpful in specification interpretations and background as part of AASHTO SCOBS T-12. Mr. Carl Macchietto and Valmont provided the test specimens at cost. The writers are responsible for the content of this paper.

### References

- American Association of State Highway and Transportation Officials (AASHTO). (2001a). *Standard specifications for structural supports for highway signs, luminaires and traffic signals*, 4th Ed., AASHTO, Washington, D.C.
- American Association of State Highway and Transportation Officials

- (AASHTO). (2001b). *Standard specifications for structural supports for highway signs, luminaires and traffic signals*, 4th Ed., AASHTO, Washington, D.C., with 2002, 2003, and 2006 interims.
- American Association of State Highway and Transportation Officials (AASHTO). (2007). *AASHTO LRFD bridge design specifications*, 4th Ed., AASHTO, Washington, D.C.
- American Association of State Highway and Transportation Officials (AASHTO). (2008). *AASHTO LRFD bridge design specifications*, Washington, D.C.
- American Institute of Steel Construction (AISC). (2001). *Manual of steel construction*, 3rd Ed., AISC, Chicago.
- The Committee on Fatigue and Fracture Reliability of the Committee on Structural Safety and Reliability of the Structural Division. (1982). "Fatigue reliability: Variable amplitude loading." *J. Struct. Div.*, 108(1), 47–69.
- Connor, R. J., and Hodgson, I. C. (2006). *Field instrumentation and testing of high-mast lighting towers in the State of Iowa*, Iowa Dept. of Transportation, Ames, IA.
- Connor, R. J., Hodgson, I. C., Ocel, J., and Brakke, B. (2005). "Fatigue cracking and inspection of high-mast lighting towers." *Paper to the International Bridge Conference*, Transportation Research Board, Washington, D.C.
- Dexter, R. J., and Ricker, M. J. (2002). "Fatigue resistant design of cantilevered signal, sign, and light supports." *NCHRP Rep. No. 469*, National Cooperative Highway Research Program, Transportation Research Board, Washington, D.C.
- Fisher, J. W., Albrecht, P. A., Yen, B. T., Klingerman, D. J., and McNamee, B. M. (1974). "Fatigue strength of steel beams with welded stiffeners and attachments." *National Cooperative Highway Research Program Rep. No. 147*, National Academy of Sciences, Washington, D.C.
- Fisher, J. W., Frank, K. H., Manfred, A. H., and McNamee, B. M. (1970). "Effect of weldments on the fatigue strength of steel beams." *National Cooperative Highway Research Program Rep. No. 102*, National Academy of Sciences, Washington, D.C.
- Frank, K. H., Budek, A., Cruzado, H., Manuel, L., and Wood, S. (2007). "Revision of AASHTO fatigue design loadings for sign, luminaires, and traffic signal structures, for use in Texas." *Project Summary Rep. No. 0-4586*, Texas Dept. of Transportation, Austin, TX.
- Hamilton, H. R., Puckett, J. A., Gray, B., Wang, P., Deschamp, B., and McManus, P. (2002a). "Traffic signal pole research final report." *Rep. to the Wyoming Dept. of Transportation*, Univ. of Wyoming, Laramie, WY.
- Hamilton, H. R., Riggs, G. S., and Puckett, J. A. (2002b). "Increased damping in cantilevered traffic signal structures." *J. Struct. Eng.*, 126(4), 530–537.
- Kaczinski, M. R., Dexter, R. J., and Van Dien, J. P. (1998). "Fatigue resistant design of cantilevered signal, sign, and light supports." *NCHRP Rep. No. 412*, National Cooperative Highway Research Program, Transportation Research Board, Washington, D.C.
- Koenigs, M. T., Botros, T. A., Freytag, D., and Frank, K. H. (2003). *Fatigue strength of signal mast arm connections*, Center for Transportation Research, Univ. of Texas at Austin, Austin, TX.
- Peiffer, J. P., Puckett, J. A., and Erikson, R. G. (2008). "Fatigue testing of ring-stiffened traffic signal structures." *Final Rep. No. FHWA-WY-08-05F*, Wyoming Dept. of Transportation, Laramie, WY.
- Sherwin. (2005). "Visible dye penetrant process: Spray can method." *Inspection manual*, Sherwin, South Gate, CA.
- WYDOT. (2005). "Specifications for fabrication of test specimens." *Design drawing*, Wyoming Dept. of Transportation, Laramie, WY.